Inelastic neutron scattering study of the ordered Pd–Ag–H hydrides

A I Kolesnikov†, V E Antonov†, G Eckold‡, M Prager§ and J Tomkinson‖

† Institute of Solid State Physics Russian Academy of Sciences, 142432 Chernogolovka, Moscow District, Russia
‡ Institut für Kristallographie, Technische Hochschule, W-5100 Aachen, Federal Republic of Germany
§ Institute für Festkörperforschung der Forschungcentrum Jülich, W-5170 Jülich, Federal Republic of Germany
‖ Rutherford Appleton Laboratory, Chilton, Didcot, Oxon OX11 0QX, UK

Abstract. Inelastic incoherent neutron scattering studies of vibrational spectra (2–400 meV) were carried out on the atomically ordered phase of palladium–silver hydrides synthesized under a high pressure of gaseous hydrogen. The results showed a large difference between the Pd–H and Ag–H interactions in the hydrides. The optic-phonon group was found to be split into two peaks. One peak was positioned at about the same energy as the peak from the transverse optic modes in PdH_x whereas the other had a much higher energy and originated from the Ag–H interaction. The experimental spectrum of nearly stoichiometric $PdAgH_{0.86}$ was fitted using a conventional Born–von Kármán model. The value of about 93 meV was predicted for the local hydrogen vibrations in dilute Ag–H solid solutions.

1. Introduction

The Pd–Ag–H hydrides are examples of the very few hydrides of disordered substitutional alloys the dynamical properties of which have been studied by the neutron scattering technique. Incoherent inelastic neutron scattering (IINS) measurements [1] have shown the position of the fundamental peak of hydrogen optic vibrations in $Pd_{0.9}Ag_{0.1}H_{0.55}$ and $Pd_{0.8}Ag_{0.2}H_{0.45}$ to be nearly the same as in $PdH_{0.68}$. According to the data of a coherent inelastic neutron scattering investigation [2], the optic peak positions in $Pd_{0.9}Ag_{0.1}D_{0.61}$ and $PdD_{0.63}$ were also close to each other, the former being only about 4% higher.

Correspondingly, it was concluded in [1, 2] that the Pd–H and Ag–H force constants are almost the same in the hydrides studied. However, one should rather expect a pronounced difference in Pd–H and Ag–H bonding, taking into account the large different between the hydrogen chemical potentials of Pd and Ag (palladium forms hydrides at $P_{H_2} < 1$ bar whereas the hydrogen solubility in silver does not exceed 0.1 at.% even at $P_{H_2} = 67$ kbar [3]).

Moreover, the observed absence of noticeable changes in the optical peak position allows another explanation. Mössbauer investigations of non-stoichiometric hydrides of many disordered alloys have revealed that the occupation probability of hydrogen for different interstitial sites depends on the actual local environments [4]. In particular, in the Pd–Au–H hydrides, there were virtually no hydrogen occupied sites next to Au atoms as long as sites having only Pd neighbours were available [4, 5]. Since Ag is a close chemical analogue of

Au, one cannot exclude the fact that most of the hydrogen atoms in the Pd–Ag–H hydrides studied in [1, 2] were located on interstitials surrounded mainly by Pd as well; consequently spectra of H vibrations were thus determined essentially by the Pd–H interaction.

The uncertainty in the interpretation of the IINS spectra could be avoided if another phase of the Pd–Ag–H system with known positions of all the constituent atoms in the crystal lattice is studied. The atomically ordered $PdAgH_{\simeq 0.9}$ hydride which is formed on the basis of a disordered FCC Pd–Ag alloy under high hydrogen pressures and elevated temperatures [3]. A neutron diffraction investigation [6] has shown that this nearly stoichiometric hydride has a primitive tetragonal cell (space group, $P4/mmm$) with $a \simeq a_0/\sqrt{2}, C \simeq a_0$, where a_0 is the cell parameter of the initial FCC Pd–Ag alloy increased by about 5% because of the hydrogen uptake. As shown in figure 1, its structure consists of layers ...–Ag–PdH–Ag–PdH... perpendicular to the tetragonal axis with the hydrogen atoms on the octahedral sites within the Pd layers. The layered structure of the hydride also provides an additional opportunity to study the effect of two-dimensional H–H interaction on the phonon spectrum.
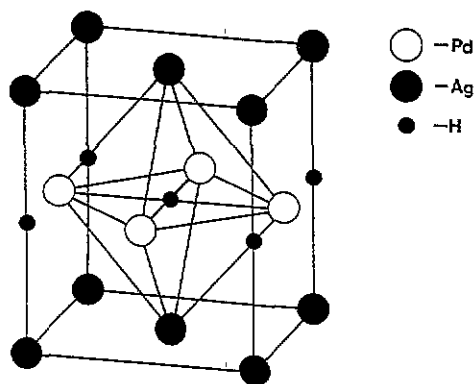

Figure 1. Crystal structure of the PdAgH ordered phase [6].

In the present work, we measured the IINS spectra of the ordered hydride $PdAgH_{0.86}$ as well as that of the hydrogen-depleted $PdAgH_{0.50}$ in order to investigate the dependence of the phonon spectrum upon the hydrogen concentration. The one-phonon spectrum derived from the experimental data on $PdAgH_{0.86}$ was then fitted to a Born–von Kármán model.

2. Experimental details

The procedures and technique used to prepare and test the $PdAgH_x$ samples were the same as in [3, 6]. The initial sample of about 3.2 g was made out of PdAg polycrystalline plates 0.3 mm thick. After hydrogenation in an atmosphere of molecular hydrogen at 28 kbar and 470 K for 24 h, it was rapidly cooled to 100 K and, in order to avoid hydrogen losses, never warmed above this temperature until the measurements were completed. The ordered hydride obtained had the composition $PdAgH_{0.86\pm0.03}$ with the cell parameters $a = 3.997/\sqrt{2}$ Å and $c = 4.270$ Å at 100 K and normal pressure. The depleted $PdAgH_{0.50\pm0.03}$ sample ($a = 3.999/\sqrt{2}$ Å; $c = 4.160$ Å) was prepared by warming $PdAgH_{0.86}$ to room temperature at atmospheric pressure for 35 h.

The IINS measurements were carried out at 24 K on the time-focused crystal analyser (TFXA) spectrometer [7] at the spallation neutron source, ISIS, Rutherford Appleton Laboratory, UK. Neutrons from a white incident beam scattered by the sample at an angle

of about 135° with an energy of 3.8 meV were analysed with a PG crystal and recorded. The spectrometer provided excellent resolution $\Delta\omega/\omega \leqslant 2\%$ and $\Delta Q \simeq 0.2$ Å^{-1}, in the range of energy transfer from 2 to 400 meV (the corresponding momentum transfer Q was energy dependent and varied from 3 to 15 Å^{-1}). The neutron transmission through the samples exceeded 90%, and multiple-scattering contributions were negligible. After the subtraction of the background determined in a separate measurement, the data were transformed to $S(Q, \omega)$ versus energy transfer (meV) using standard programs.

The contributions from the multiphonon neutron scattering (up to four-phonon processes) were calculated in a harmonic isotropic approximation by the multiconvolution of the one-phonon spectrum using an interative technique [8, 9]. Experimental data in the energy range of the lattice and hydrogen optic phonons, 2–115 meV, were used at the first interative step as the one-phonon spectrum of hydrogen vibrations. On the second and subsequent steps, the one-phonon spectrum was assumed to be the difference between the experimental spectrum and that resulting from the multiphonon processes; convergence was achieved in three iterations.
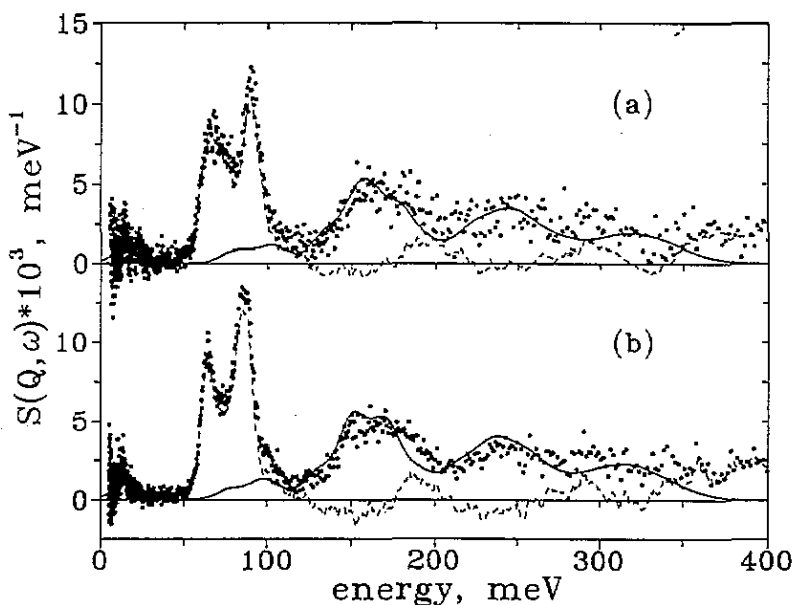

Figure 2. The IINS spectra $S(Q, \omega)$ (●) for (a) PdAgH$_{0.50}$ and (b) PdAgH$_{0.86}$ as measured on the TFXA at 24 K: ——, calculated multiphonon contributions; – – –, one-phonon spectra.

3. Results

Figure 2 shows the experimental IINS spectra $S(Q, \omega)$ (full circles) and calculated one-phonon (broken curves) and multiphonon (full curves) neutron scattering contributions for the palladium–silver hydrides.

The contribution of multiphonon processes to the spectra of lattice vibrations (which cut off at about 25 meV) was negligible. The smoothed curves of $S(Q, \omega)$ spectra in figure 3 display, more or less clearly, a peak at 13–14 meV and two doubtful peaks at 6–9 and
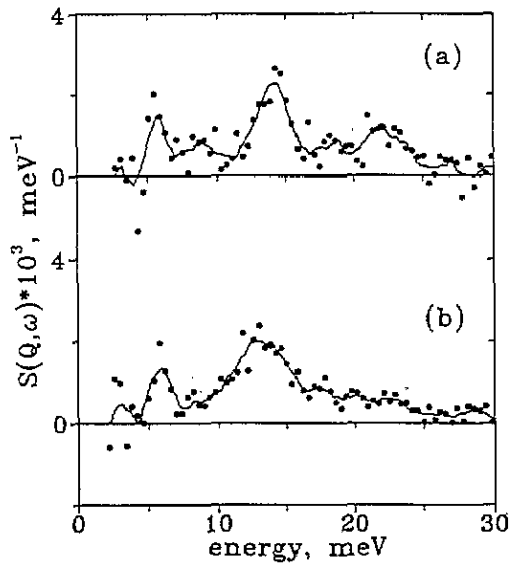
Figure 3. The INS spectra $S(Q, \omega)$ (●) in the region of metal lattice vibrations for (a) $PdAgH_{0.50}$ and (b) $PdAgH_{0.86}$ (in view of the poor statistics in this energy region, the points were obtained by integrating the experimental data over energy intervals $\Delta\omega = 0.4$ meV): ——, the results of smoothing by a polynomial of second order.

22 meV. The presence of peaks at 13–14 and 22 meV agrees with the available data for PdH_x [10–12] and for $Pd_{1-y}Ag_yH_x$ [13]. As for the possible leftmost peak, peculiarities at 6–9 meV were also observed in the PdH_x spectrum in [9, 13], but nothing was detected in this part of phonon spectra for Pd, PdH $(D,T)_x$ and Pd–Ag–D in [2, 10, 14–17]. The nature of this peak (if any) is not clear. Note that a peak at about 2–7 meV was also observed in the spectra of titanium hydrides obtained by quenching under a high pressure [18]. The range of hydrogen optic phonon spectra of our $PdAgH_x$ samples and, for comparison, that of PdH measured recently on the TFXA [12] are presented in figure 4.

The INS spectra of PdH_x [1, 9, 12, 19–22] show one optic vibrational peak (transverse optic modes) with a strong shoulder at higher energies originating from dispersion caused by the H–H interaction (longitudinal optic modes). In the case of $PdAgH_x$, the fundamental peak of hydrogen vibrations (50–115 meV) is apparently split into two lines. In order to compare the spectra in figure 4 more quantitatively, each of them was treated as a sum of three Gaussians. The parameters of the Gaussians are listed in table 1.

Table 1. Peak positions ω_i and full widths at half-maximum δ_i and peak amplitudes H_i for the optic bans of INS spectra of powder PdH [12] and ordered $PdAgH_x$ samples.

	Powder PdH			$PdAgH_{0.86}$			$PdAgH_{0.50}$		
	$i = 1$	$i = 2$	$i = 3$	$i = 1$	$i = 2$	$i = 3$	$i = 1$	$i = 2$	$i = 3$
ω_i	55.8	58.0	78.5	63.0	70.5	85.9	64.4	74.8	89.9
δ_i (meV)	4.8	11.6	22.8	7.0	16.0	11.8	11.2	11.2	12.5
H_i (arbitrary units)	324	75	48	88	75	171	104	77	141

The value of the peak frequency ω_1 in the Pd–H system is known to depend strongly upon the hydrogen concentration, decreasing from about 66–69 meV for the dilute Pd–H
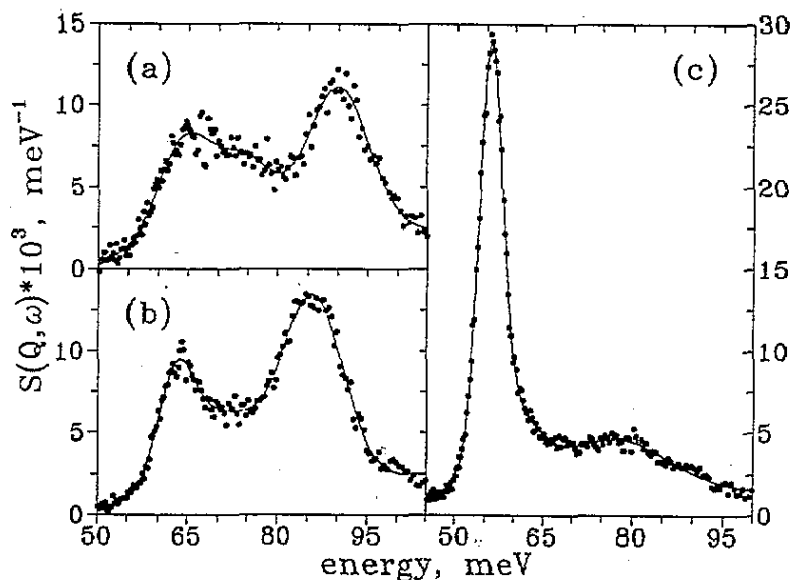
Figure 4. The INS spectra $S(Q, \omega)$ (●) for (a) $PdAgH_{0.50}$, (b) $PdAgH_{0.86}$ and (c) PdH: ——, fits with three Gaussians (see table 1).
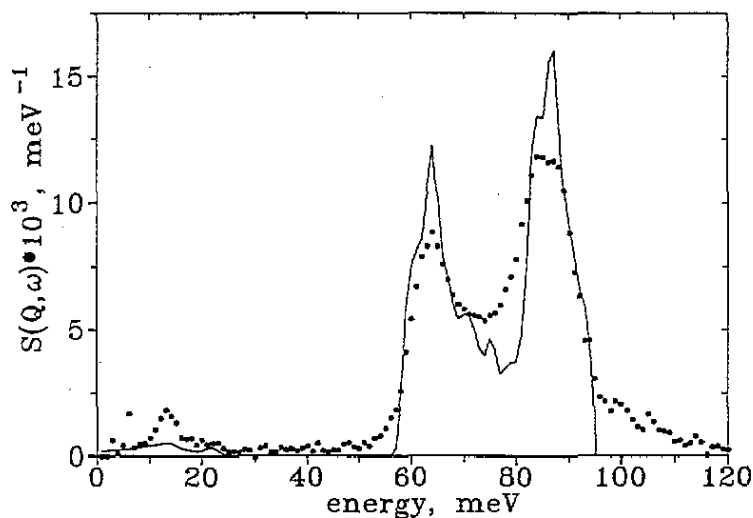

Figure 5. The one-phonon spectrum (● (spaced by 1 meV)) obtained from experimental INS data for ordered $PdAgH_{0.86}$ (broken curve in figure 2(b)) and the calculated spectrum (——) after a convolution with the model resolution function for the TFXA spectrometer taken as a triangle with the width $\Delta E = 0.02\omega$ at half-maximum.

solutions [21, 22] to about 55 meV for nearly stoichiometric PdH [1, 9, 12, 19–20]. This decrease is mainly caused by weakening of the Pd–H interaction with increasing hydrogen concentration due to an increase in the Pd–H distances ($T = 100$ K, the parameter of the PdH_x FCC cell increases from $a = 3.889$ Å for $x = 0$ to $a \simeq 4.095$ Å for $x \simeq 1$).

The values of ω_1 and ω_3 for the $PdAgH_x$ samples reflect the positions of the left-hand

and right-hand peaks, respectively, in their spectra in figure 4. As can be seen from table 1, ω_1-values for both samples lie in the energy interval characteristic of the optic peak for the palladium hydrides with intermediate hydrogen concentrations. The Pd–H distances in Pd–H planes of the PdAgH$_x$ hydrides ($a = 3.997/\sqrt{2}$ Å at $x = 0.86$ and $a = 3.999/\sqrt{2}$ Å at $x = 0.50$) are also close to those in palladium hydrides. This allows us to conclude that the left-hand optic peaks in the spectra of the PdAgH$_x$ hydrides (figures 4(a) and 4(b)) are mainly associated with the H vibrations in the Pd–H planes (in the spectrum of the palladium hydride, such a peak originates mostly from the transverse modes [10]).

This conclusion also agrees with the fact that the difference between ω_1-values for the PdAgH$_{0.86}$ and PdAgH$_{0.50}$ samples with nearly coinciding Pd–H distances is much smaller than between the ω_3-values. As for the ω_3-values, an increase in ω_3 by about 4 meV with x decreasing from 0.86 to 0.50 is reasonably ascribed to the shortening of the Ag–H distances (the parameters decreased from 4.270 to 4.160 Å). This suggests that the right-hand optic peaks in figures 4(a) and 4(b) should mainly originate from the H vibrations perpendicular to the Pd–H and Ag planes (another noticeable contribution to these peaks should be the shoulders of the left-hand peaks stretching over large energy intervals as observed for PdH in figure 4(c)).

The splitting of the optic peak in the IINS spacer of the PdAgH$_x$ hydrides is thus indicative of an appreciable difference between the Pd–H and Ag–H interactions. Assuming that firstly the ω_3-values of our PdAgH$_x$ samples are mainly determined by the Ag–H interaction, secondly the frequency of hydrogen optic vibrations in Pd–Ag alloy increases linearly with decreasing hydrogen concentration just as in Pd [15] and thirdly the Ag–H distance decreases linearly [3], one could extrapolate a value of $\omega \simeq 93$ meV for the frequency of the hydrogen optic mode in dilute solid solutions of hydrogen in FCC Ag ($a \simeq 4.074$ Å at 100 K).

In the multiphonon regime at frequencies $\omega > 125$ meV the calculated two-phonon and three-phonon bands represent the main experimental features quite well, as shown in figure 2. Note that even a fine structure of the two-phonon bands is well reproduced by the harmonic approximation calculations.

A strong anisotropy of the high-energy part ($\omega > 100$ meV) of the IINS spectra was found recently for PdH [12] while studying the sample prepared from cold-rolled palladium plates with a strong texture. Our PdAgH$_x$ samples also exhibited a strong texture. To check whether the spectrum of the PdAgH$_{0.86}$ sample is anisotropic or not, we repeated the IINS measurement on this hydride but changed the angle between the sample surface and the incident neutron momentum vector (this is always very close to the direction of the neutron momentum transfer vector owing to the low final neutron energy). The angle was changed from 90° to 45°. The spectra measured at both angles nearly coincided over the whole region of energy transfers. Hence, no anisotropy could be detected in the phonon spectra of PdAgH$_{0.86}$.

4. Model calculations

A Born–von Kármán model was applied to describe the phonon spectrum of ordered nearly stoichiometric PdAgH$_{0.86}$, and we used the UNISOFT program [23] for the calculations.

In principle, it is a rather uncertain task to fit a calculated phonon spectrum to the measured IINS spectrum because there are too many independent variables. In our case the situation seems to be less embarrassing, since the phonon dispersion curve and density of phonon states for PdH(D,T) are well studied both experimentally and theoretically

[1, 9, 10, 12, 15, 16, 19, 20]. Our experimental data allow us to assume that the Pd–H force constants in $PdAgH_{0.86}$ are close to those in PdH and that the position of the optic peak at about 86 meV is mainly determined by the Ag–H interaction.

To simplify the problem, we made the calculations for the stoichiometric hydride PdAgH. By analogy with the calculation of the phonon spectra for stoichiometric PdH [10] and non-stoichiometric $PdH_{0.63}$ [20], one could expect this simplification to result in a more structured spectrum with a higher intensity at the first hydrogen optic peak.

Under the usual assumption that the forces are central, the number of parameters for each pair atom interaction is reduced to two, namely the longitudinal force constant $L = a^2 V/ar^2$ and the transverse force constants $T = (1/r)(aV/ar)$, where V is the potential of pair interaction and r is the interatomic distance. To reduce further the number of fitting parameters, we used the same force constants for the Pd–Pd, Pd–Ag and Ag–Ag interactions. (The differences in these constants are essential in the acoustic part of the spectrum but this is beyond the scope of the present paper owing to the poor quality of the data at low frequencies (figure 3).) Interactions betweeen the atoms up to the second-neighbour shell were included in the calculations. No H–H interaction along the c axis was taken into account.

The 12 remaining adjustable force constants have been used to calculate

(1) the phonon dispersion curves in some symmetry directions of the Brillouin zone,
(2) the normalized phonon density of states given by

$$Z(\omega) = \frac{1}{3N} \sum_{j,q} \delta(\omega - \omega_j(q)) \tag{1}$$

(3) the partial weighted densities of phonon states given by

$$G_i(\omega) = \frac{1}{3Nm_i} \sum_{j,q} |e(i|qj)\delta(\omega - \omega_j(q))|^2 \tag{2}$$

and their projections on the c axis and the a–b plane, respectively.

$\omega_j(q)$ and $e(i/qj)$ are the eigenvalue and eigenvector (of atom i) of the dynamical matrix corresponding to the phonon state qj. The summation extended over $N = 6859$ points, distributed uniformly over a reduced Brillouin zone q-space.

To compare the calculated data with the experimental spectrum, we then transformed them to

$$S(Q, \omega) = \sum_i^1 f_i b_i S_i(Q, \omega) \tag{3}$$

where f_i and b_i are the atomic fraction and neutron scattering cross section for atom i and

$$S_i(Q, \omega) = (\hbar Q^2/6\omega) \exp(-Q^2 \langle u_i^2 \rangle) G_i(\omega)[n(\omega) + 1] \tag{4}$$

where $\langle u_i^2 \rangle$ is the mean square amplitude of particle i and $n(\omega)$ is the Bose factor. Because of the anisotropy of the structure and, hence, of the dynamics in PdAgH, we have calculated the $\langle u_i^2 \rangle$ values for the c direction and for the a–b plane separately:

$$\langle (u_i^c)^2 \rangle = \int \frac{\hbar}{4\omega} G_i^c(\omega)[2n(\omega) + 1]\, d\omega \tag{5}$$

and

$$\langle (u_i^{a-b})^2 \rangle = \int \frac{\hbar}{8\omega} G_i^{a-b}(\omega)[2n(\omega) + 1]\,d\omega. \tag{6}$$

The calculated $S(Q, \omega)$ spectrum was fitted to the one-phonon spectrum obtained from the experimental IINS data for the $PdAgH_{0.86}$ sample by a test-and-trial method. The parameters of the experimental spectrum to be reproduced were the positions and relative intensities of the two peaks of hydrogen optic vibrations. The results of our best fit are presented in figure 5, the force constants used are listed in table 2.

Table 2. The longitudinal force constants L and transverse force constants T used for the calculations.

	First neighbour		Second neighbour	
	L	T	L	T
Pd–Pd($\equiv$Ag–Ag)	32.00	−3.40	−0.50	0.65
Pd–Ag	32.00	−3.40		
H–H	3.55	−1.05	1.90	−0.17
Pd–H	1.30	0.95		
Ag–H	15.50	4.40		

The calculations do not pretend to describe thoroughly all the details of the dynamics of $PdAgH_{0.86}$ but, judging by the reasonable values of the obtained force constants, ought to outline its general features.
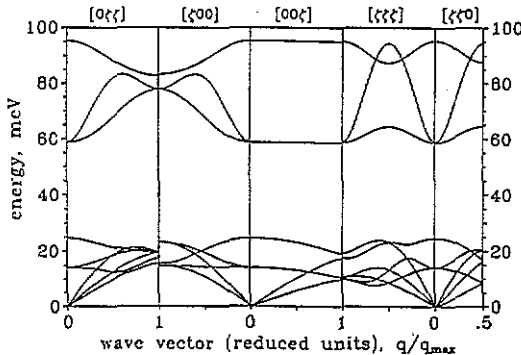

Figure 6. Phonon dispersion curves in ordered PdAgH. The curves are calculated on the basis of the Born–von Kármán model with the 12 parameters listed in table 2.

5. Discussion of the calculated data

Figure 6 presents the phonon dispersion curves for the PdAgH crystal calculated with the force constants from table 2. The curves are more complicated than those known for PdH
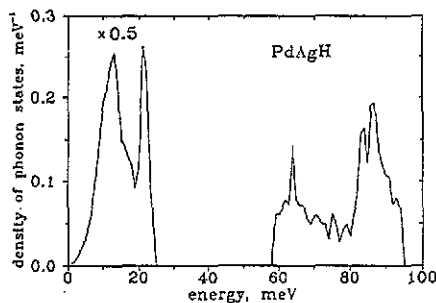
Figure 7. Calculated phonon density $Z(\omega)$ of states for PdAgH.

since the maximum number of phonon branches here is nine because the unit cell contains three atoms instead of two.

At low energies ($\omega < 25$ meV), the dynamics are mainly determined by vibrations of the two heavier atoms, Pd and Ag, with approximately the same atomic masses ($m_{Pd} = 106.42$ au and $m_{Ag} = 107.90$ au). This region consists of three acoustic and three optic modes and differs noticeably from that for the Pd and PdH crystals [10, 14, 16]. Nevertheless, the resultant density of phonon states of PdAgH in this energy interval (figure 7) looks similar to that of PdH_x obtained earlier [10, 12]. This is to be expected since we set the metal–metal force parameters equal to that of the Pd–Pd interaction.

In the range of hydrogen optic vibrations ($\omega > 55$ meV (figure 6)), the two lower phonon modes display rather high dispersions whereas the dispersion of the third higher-energy mode is much smaller. A specific feature of all the hydrogen optic modes is the absence of any dispersion in the [00ξ] direction. This is a consequence of the nearly two-dimensional character of the H–H interaction due to a long distance between the H atoms along c that allowed us to neglect their interaction in the calculations.

Figures 8 and 9 show the calculated spectra of partial weighted densities $G_i(\omega)$ of phonon states, and the calculated IINS spectra $S_i(Q, \omega)$, respectively. The full curves represent the projections of $G_i(\omega)$ and $S_i(Q, \omega)$ on the a–b plane and the broken curves the projections on the c axis. The upper spectra in figures 8 and 9 present the corresponding sums over all the atoms with their scattering amplitudes (see equation (3)) and atomic fractions taken into account.

At low energies ($\omega < 25$ meV), the only difference in $G_i(\omega)$ for the Pd and Ag atoms is that the first peak in $G_{Ag}^c(\omega)$ has a slightly higher energy position. The form of $G_H^c(\omega)$ is close to that for the Ag atoms. In the a–b plane, however, the H atoms exhibit a different behaviour. The first peak in $G_H^{a-b}(\omega)$ is positioned at about 8 meV and the low-energy asymptote for $G_H^{a-b}(\omega)$ does not follow the Debye law $G(\omega) \propto \omega^2$ (this law results in an unusual $S_H^{a-b}(Q, \omega)$ dependence; see figure 9).

According to our model calculations (figure 10), the a–b projection of the hydrogen phonon eigenvector amplitude for the acoustic modes increases strongly with q approaching the centre of the Brillouin zone. The corresponding amplitudes for the H vibrations along the c axis as well as those for the metal atom vibrations in all directions vary only slightly. We suppose that the peculiar behaviour of hydrogen vibrations in the a–b plane is due to a two-dimensional character of the H–H interaction in the crystal.

In the region of hydrogen optic modes, as is seen from figure 9, the peak at around 86 meV originates mainly from the H vibrations along the c axis, and no H vibrations in
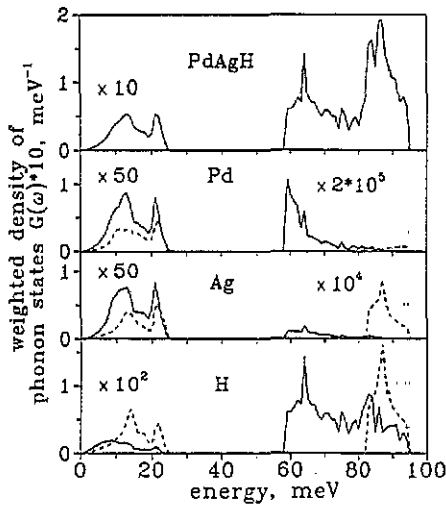
Figure 8. Calculated total weighted density $G(\omega)$ of phonon states for ordered PdAgH (upper spectrum) and the projections on the c axis (– – –) and a–b plane (——) of partial weighted densities of phonon states for Pd, Ad and H atoms. Note the different scales for different ranges of spectra.
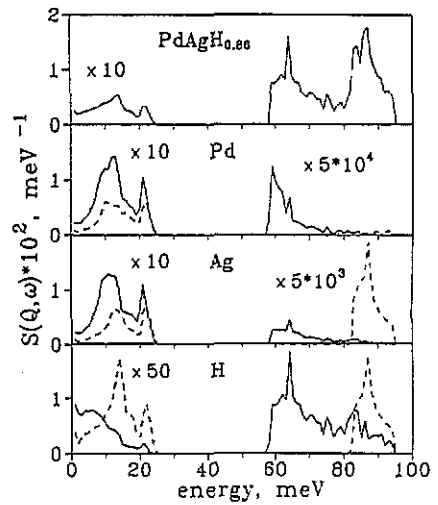
Figure 9. Calculated total IINS spectrum for ordered PdAgH$_{0.86}$ (upper spectrum, arbitrary units) and projections of contributions to the IINS spectrum from Pd, Ag and H atoms on the c axis (– – –) and a–b plane (——). The spectra are obtained from the data in figure 8 by means of equations (3) and (4), respectively.
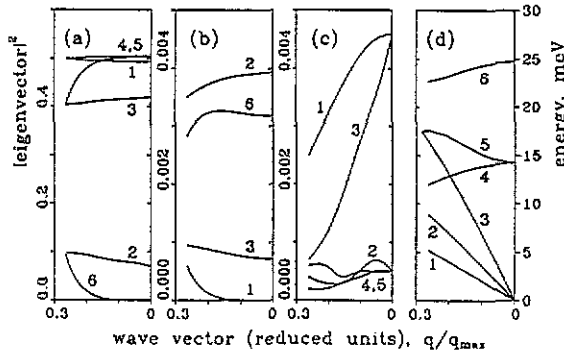

Figure 10. Calculated squared amplitudes of phonon eigenvectors along $[\zeta\zeta\zeta]$ versus q near to the centre of the PdAgH Brillouin zone: (a) a–b projection, Pd atoms (dependences for Ag atoms are approximately the same); (b) c axis projection, H atoms; (c) a–b projection, H atoms; (d) corresponding phonon dispersion curves (from figure 6). The numerals indicate different phonon modes; eigenvector amplitudes for some modes which are not shown in (b) and (c) are negligible.

this direction exist at energies less than 81 meV. Contrary to this, H vibrations in the a–b plane cover the whole energy region of H optic modes from 58 to 94 meV.

Furthermore, the results of the model calculations allow us to analyse contributions from the metal atoms to the hydrogen optic modes which cannot be detected in the IINS experiments. One can see from figure 8 that, for c axis vibrations, the Pd atoms exhibit a much smaller weighted density of states than the Ag atoms. The Pd atoms are almost not involved in the vibrations along the c axis whereas the Ag atoms vibrate predominantly in this very direction.

The calculated and experimental spectra are compared in figure 5. Obviously, quantitative agreement is not achieved. The most essential discrepancy is that the calculated intensities in the low-energy part of the spectrum ($\omega < 25$ meV) are approximately 2.5 times smaller than the experimental values (in spite of the poor statistics of the measured spectrum in this energy region the discrepancy is clearly out of the range of

experimental uncertainties). We suppose that it is due to underestimated values of the mean square displacement of hydrogen atoms (table 3) entering the Debye–Waller factor in equation (4). Calculated values of the hydrogen mean square amplitudes much smaller than the experimental values seem to be rather typical for the calculations of the hydride dynamics and have been reported, for example, for hydrogen in palladium [24], niobium [25, 26] and vanadium [27].

Table 3. Calculated mean square displacement $\langle u_i^2 \rangle$ of atom i in PdAgH at 24 K for different directions.

| Atom | $\langle u_i^2 \rangle (10^{-3}$ Å^2) | |
	a–b plane	c axis
Pd	0.42	0.37
Ag	0.41	0.34
H	6.74	5.70

Moreover, one can see from figure 5 that the calculated spectrum does not fit the shoulders of the hydrogen optic peaks. The obvious reason is that the calculations were done for the hydride of stoichiometric composition PdAgH while the experimental spectrum was measured on non-stoichiometric PdAgH$_{0.86}$; see [20] where the analogous case of non-stoichiometric PdH$_{0.63}$ was considered in detail.

6. Conclusions

The IINS spectra were measured for the ordered PdAgH$_x$ hydrides. The experimental results for the first time clearly show a large difference between the Pd–H and Ag–H interactions. This formally contradicts the data of dynamical studies on the Pd–Ag hydrides with a disordered metal lattice [1, 2] which have shown only a weak influence of Ag on the vibrational spectra of palladium hydrides. The results of [1, 2] can be explained if one suggests that the hydrogen atoms in the disordered Pd–Ag alloys as well as in the analogous Pd–Au alloys [4, 5] occupy preferentially interstitial sites surrounded mainly by palladium atoms.

The Born–von Kármán model calculations of the phonon spectrum carried out for ordered PdAgH permitted a reasonably good description of the measured IINS spectrum of PdAgH$_{0.86}$. The projection of the calculated weighted density $G_H^{a-b}(\omega)$ of phonon states for hydrogen atoms on the a–b plane showed an anomalous non-Debye behaviour at low energies, probably caused by the two-dimensional character of the H–H interaction in the crystal.

Acknowledgments

References

[1]   Chowdhury M R and Ross D K 1973 *Solid State Commun.* **13** 229–34
[2]   Fratz P, Blaschko O and Walker E 1986 *Phys. Rev.* B **34** 164–8
[3]   Antonov V E, Antonova T E, Belash I T and Ponyatovsky E G 1984 *Fiz. Metall. Metalloved.* **57** 671–9
[4]   Karger M, Pröbst F, Schüttler B and Wagner F E 1982 *Metal–Hydrogen Systems* ed T N Veziroglu (Oxford: Pergamon) pp 131–67
[5]   Baier M *et al* 1992 *Z. Phys. Chem.* at press
[6]   Irodova A V, Glazkov V P, Somenkov V A, Antonov V E and Ponyatovsky E G 1989 *Z. Phys. Chem. NF* **163** 53–7
[7]   Penfold J and Tomkinson J 1986 *Rutherford Appleton Laboratory Internal Report* RAL-86-019
[8]   Antonov V E, Belash I T, Kolesnikov A I, Maier J, Natkaniec I, Ponyatovskii E G and Fedotov V K 1991 *Sov. Phys.–Solid State* **33** 87–90
[9]   Kolesnikov A I, Natkaniec I, Antonov V E, Belash I T, Fedotov V K, Krawczyk J, Mayer J and Ponyatovsky E G 1991 *Physica* B **174** 257–61
[10] Rowe J M, Rush J J, Smith H G, Mostoller Mark and Flotow H E 1974 *Phys. Rev. Lett.* **33** 1297–300
[11] Schober H R and Lottner V 1979 *Z. Phys. Chem. NF* **114** 203–12
[12] Kolesnikov A I, Antonov V E, Bokhenkov E L and Ross D K 1993 *ISIS Annual Report 1991* p A293 (to be published)
[13] Chowdhury M R 1974 *J. Phys. F: Met. Phys.* **4** 1657–64
[14] Miller A P and Brockhouse B N 1971 *Can. J. Phys.* **49** 704–23
[15] Blaschko O, Klemencic R, Weinzierl P and Pintschovious L 1981 *Phys. Rev.* B **24** 1552–5
[16] Glinka C J, Rowe J M, Rush J J, Rahman A, Sinha S K and Flotow H E 1978 *Phys. Rev.* B **17** 488–93
[17] Rowe J M, Rush J J, Schirber J E and Mintz J M 1986 *Phys. Rev. Lett.* **57** 2955–8
[18] Kolesnikow A I, Monkenbusch M, Prager M, Bashkin I O, Malyshev V Yu and Ponyatovskii E G 1989 *Z. Phys. Chem. NF* **163** 709–14
[19] Ross D K, Martin P F, Oates W A and Khoda Bakhsh R 1979 *Z. Phys. Chem. NF* **114** 221–30
[20] Rahman A, Sköld K, Pelizzari C, Sinha S K and Flotow H 1976 *Phys. Rev.* B **14** 3630–4
[21] Drexel W, Murani A, Tocchetti D, Kley W, Sosnowska I and Ross D K 1976 *J. Phys. Chem. Solids* **37** 1135–9
[22] Rush J J, Rowe J M and Richter D 1984 *Z. Phys.* B **55** 283–6
[23] Eckold G, Stein-Arsic M and Weber H-J 1986 *UNISOFT—A Program Package for Lattice-Dynamical Calculations: User Manual* (Jülich: IFF KFA)
[24] Sköld K and Nelin G 1967 *J. Phys. Chem. Solids* **28** 2369–80
[25] Gissler W, Alefeld G and Springer T 1970 *J. Phys. Chem. Solids* **31** 2361–9
[26] Wakabayashi N, Alefeld B, Kehr K W and Springer T 1974 *Solid State Commun.* **15** 503–6
[27] Rowe J M, Sköld K, Flotow H E and Rush J J 1971 *J. Phys. Chem. Solids* **32** 41–54